Radiocarbon, Vol 65, Nr 4, 2023, p 967–978 DOI:10.1017/RDC.2023.66


# SPATIAL DISTRIBUTION OF FOSSIL FUEL $CO_2$ IN MEGACITY DELHI DETERMINED USING RADIOCARBON MEASUREMENTS IN PEEPAL (*FICUS RELIGIOSA*) TREE LEAVES

Rajveer Sharma[1,2*] • Ravi Kumar Kunchala[2*] • Sunil Ojha[1] • Pankaj Kumar[1] • Deeksha Khandelwal[1] • Satinath Gargari[1] • Sundeep Chopra[1]

[1]Inter University Accelerator Centre, New Delhi 110067, India
[2]Centre for Atmospheric Sciences, Indian Institute of Technology Delhi, New Delhi 110016, India

**ABSTRACT.** The quantification of fossil-fuel derived carbon dioxide ($CO_{2ff}$) emissions is critical for regional carbon budgets. Radiocarbon ($^{14}C$) is an effective tool to estimate the contribution of $CO_{2ff}$ to the total atmospheric $CO_2$. In the present study, we have determined the spatial distribution of fossil fuel derived $CO_2$ across Delhi using $^{14}C$ measurements in Peepal tree leaves from April 2016 to March 2017 at city scale. Our analysis results show that the $\Delta^{14}C$ values vary between –67.78‰ to 5.61‰ and corresponding $CO_{2ff}$ values are varying from 1.63 ppm to 33.34 ppm. $CO_{2ff}$ values from campus sites vary between 6.99 ppm to 16.38 ppm with an average value of 10.22 ± 3.20 ppm, while $CO_{2ff}$ values vary from 2.41 ppm to 33.34 ppm with an average value of 13.32 ± 9.40 ppm for sites located in the parks. Further, we observed the higher contributions of fossil fuels in the $CO_2$ from northwest Delhi, central Delhi, and some parts of east and southwest Delhi. In the absence of real-time $CO_2$ monitoring, the results of this study provide a potential method for analyzing the contribution of $CO_{2ff}$ values over the urban landscape to total $CO_2$ over the study region.

**KEYWORDS:** fossil fuel carbon dioxide ($CO_{2ff}$), greenhouse gas, radiocarbon, urban emissions.

## INTRODUCTION

The rising levels of carbon dioxide ($CO_2$) in the atmosphere due to an increase in the anthropogenic fossil fuel burning activities are leading to climate change (IPCC 2014; Le Quéré et al. 2018). $CO_2$ mole fractions in the atmosphere have increased from 280 parts per million (ppm) before the industrial revolution to 415.7 ppm in 2021, which is approximately 49% higher than preindustrial $CO_2$ concentrations (WMO 2022). Further, cities and urban areas are responsible for 70% of this increase (Duren and Miller 2012; Seto et al. 2014). The primary reason for this increase in $CO_2$ emissions is the burning of fossil fuels (Boden et al. 2010). $CO_2$ emitted by combustion of fossil fuels is an additional flux in the atmosphere that perturbs the natural flux of $CO_2$ and leads to increase the $CO_2$ levels in the atmosphere (Ciais et al. 2013; Turnbull et al. 2016). As a result, understanding the contribution of fossil fuel $CO_2$ ($CO_{2ff}$) emissions from cities and urban areas is critical to develop an effective mitigation policy (Wang et al. 2021). Typically, fossil fuel $CO_2$ ($CO_{2ff}$) emissions are calculated using fuel consumption data, but this method has large estimation errors at fine spatial resolutions (Marland et al. 2003; Andres et al. 2012). To overcome the shortcomings of this method, as an alternative, radiocarbon ($^{14}C$) is used to trace the $CO_{2ff}$ because it is fully depleted in fossil fuels. Therefore, $CO_{2ff}$ can easily be identified from other sources based on its radiocarbon content (Levin et al. 2003).

$^{14}C$ content is generally measured in air samples collected in flask (Turnbull et al. 2006) and air bags (Niu et al. 2016a) or over sodium hydroxide solution (Levin et al. 2003; Turnbull et al. 2017). Annual crop plants, grasses and tree leaves also provide a radiocarbon signal of their growing period because they absorb atmospheric $CO_2$ by photosynthesis processes (Hsueh et al. 2007; Riley et al. 2008; Bozhinova et al. 2016; Niu et al. 2016b; Varga et al. 2020a). However, because crop plants are not found in cities, tree leaves and grasses are the best plant

*Corresponding authors. Emails: rajveersharma1988@gmail.com; rkkunchala@cas.iitd.ac.in

samples to study the spatial variation of $CO_{2ff}$ across cities and urban areas (Riley et al. 2008; Niu et al. 2016b; Varga et al. 2019, 2020a). Several radiocarbon-based studies have been carried out in various cities and urban areas around the world to quantify $CO_{2ff}$ contribution (Lichtfouse et al. 2005; Riley et al. 2008; Wang and Pataki 2010; Park et al. 2013; Niu et al. 2016b; Santos et al. 2019; Varga et al. 2020a; Zhou et al. 2020).

India is the third largest $CO_2$ emitter (Friedlingstein et. al. 2020) and home to the second largest urban population in the world (UN 2014). In 2011, 32% of the population of India is living in the urban areas, and it is further expected to grow up to 50% by 2050 (UN 2014; Ahmed et al. 2015). Furthermore, India's current urban population is 10.5 percent of the global urban population, with a projected increase to 12.8 percent by 2050 (UN 2014; Ahmed et al. 2015). Therefore, study of $CO_2$ emissions from Indian cities and urban areas is not only useful to make mitigation policies for India but also for its global implications.

Several studies based on atmospheric $CO_2$ observations have been documented over the Indian region, including Indian cities, urban and semi-urban areas (Tiwari et al. 2013, 2014; Lal et al. 2015; Lin et al. 2015; Chandra et. al. 2016; Sharma et al. 2014; Sreenivas et. al. 2016; Jain et al. 2021; Metya et. al. 2021). A recent study of fossil fuel $CO_2$ estimation based on radiocarbon measurements in crop plants across India has also been reported (Sharma et al. 2023). However, to the best of our knowledge, no $^{14}C$-based $CO_{2ff}$ measurements have been reported from any Indian city. Therefore, in this study, we used $^{14}C$ measurements from Peepal tree leaves to determine spatial variations of $CO_{2ff}$ in the megacity of Delhi.

## MATERIAL AND METHODS

### Study Area

Delhi is India's capital city and is governed as a national capital territory (NCT). Delhi is also one of the most polluted cities in the world (WHO 2016; Mahato et al. 2020) and the world's second most populous megacity (UN 2018; Mahato et al. 2020). The megacity Delhi (28°22′N to 28°54′N latitude and 76°50′E to 77°20′E longitude) covers an area of 1483 $km^2$ geographically. Haryana and Uttar Pradesh states are neighboring states of megacity Delhi surrounding it from three sides (north, east, south) and one side (west), respectively. The topography of megacity Delhi can be divided into three major zones: the Yamuna floodplains, the Aravalli Ridge, and the great Gangetic plains (isfr vol. 2, 2019). However, the main portion of the megacity is covered by the Gangetic plain, having an elevation in the range of 180–316 m above mean sea level (isfr vol. 2, 2019). It is also reported that the population of Delhi is 16.8 million with a density of 11,320 per square km and 97.5% urban and 2.5% rural population as per the 2011 census (Census 2011; http://census2011.co.in). Delhi's climate is semi-arid with an annual average temperature of 31.5°C (Masood et. al. 2023) and rainfall ranging from 400 mm to 600 mm (isfr vol. 2, 2019), and the prevailing wind direction is northwest. The total number of registered vehicles in Delhi was 12.25 million by 2021 (Delhi Economic Survey 2021–2022), and this number is expected to increase up to 25.6 million by 2030 (Kumar et al. 2017). The national capital region (NCR) includes the megacity of Delhi as well as its neighboring cities of Gurgaon, Faridabad, Noida, Ghaziabad, Sonipat, and Bahadurgarh (Mahato et al. 2020). As shown in Figure 1, Delhi city is also home to several industrial units, two coal-fired thermal power plants, and three gas-fired power plants.

Table 1 List of locations of samples with sampling year, latitude, longitude, measured $\Delta^{14}C$ values, associated uncertainty, adjusted $\Delta^{14}C$ values to 2017, and calculated $CO_{2ff}$ values.

| S. no. | Sample ID | Location code | Location (sampling year) | Lat./Long. | Site description | $\Delta^{14}C$ (‰) | Uncertainty | $\Delta^{14}C$ adjusted to 2017 | $CO_{2ff}$ (ppm) |
|---|---|---|---|---|---|---|---|---|---|
| 1 | IUACD#20C3004 | CDL | Central Delhi, Near Mandi House Metro Station (2017) | 28°37′20.388″N, 77°13′50.724″E | Site near various offices | –47.17 | 2.37 | | 23.94 |
| 2 | IUACD#20C3006 | KSA | Khalsa College (2017) | 28°41′48.48″N, 77°12′33.47″E | Campus site | –7.59 | 2.26 | | 6.99 |
| 3 | IUACD#20C3008 | DWK1 | Dwarka Sector 12 (2017) | 28°35′47.78″N, 77°02′31.77″E | Site near different institutions | –0.07 | 2.19 | | 3.92 |
| 4. | IUACD#20C3010 | SSP | Bhagat Singh Park, Geeta Colony (2017) | 28°38′49.92″N, 77°16′30.91″E | Park site | –67.78 | 2.13 | | 33.34 |
| 5 | IUACD#20C3012 | DWK2 | Dwarka Sector 16 (2017) | 28°36′01.99″N, 77°01′17.89″E | Site in a residential area | –15.40 | 1.93 | | 10.23 |
| 6 | IUACD#20C3013 | DU2 | Delhi University (2017) | 28°41′22.632″N, 77°12′38.16″E | Campus site | –13.59 | 1.99 | | 9.47 |
| 7 | IUACD#20C3016 | VJN | Kalyan Vihar (2017) | 28°41′26.41″N, 77°11′57.52″E | Park in residential area | –5.64 | 1.99 | | 6.19 |
| 8 | IUACD#20C3017 | NZF | Deenpur, Nazafgarh (2017) | 28°35′25.21″N, 76°59′57.47″E | Park site | –25.31 | 1.95 | | 14.41 |
| 9 | IUACD#20C3018 | RON | Roopnagar (2017) | 28°41′10.19″N, 77°12′06.33″E | Park in residential area | –27.12 | 2.09 | | 15.18 |
| 10 | IUACD#20C3020 | SDG | Safadarganj (2017) | 28°35′15.06″N, 77°12′45.01″E | Site near a road and monument | –9.48 | 1.97 | | 7.77 |
| 11 | IUACD#20C3021 | HRN | Hari Nagar (2017) | 28°37′07.70″N, 77°06′24.08″E | Park site | 3.66 | 2.08 | | 2.41 |
| 12 | IUACD#20C3023 | CHK | Chandani Chawk (2017) | 28°39′25.10″N, 77°13′46.55″E | Park site near a market | –7.25 | 1.98 | | 6.85 |
| 13 | IUACD#20C3024 | MLP | Mngolpuri, North West Delhi (2017) | 28°41′45.24″N, 77°05′44.17″E | Local market | –27.85 | 1.78 | | 15.49 |
| 14 | IUACD#20C3033 | VKP | Vikaspuri (2017) | 28°38′09.83″N, 77°04′27.81″E | Park site | –26.30 | 1.99 | | 14.83 |

*(Continued)*

https://doi.org/10.1017/RDC.2023.66 Published online by Cambridge University Press

Table 1 (*Continued*)

| S. no. | Sample ID | Location code | Location (sampling year) | Lat./Long. | Site description | $\Delta^{14}C$ (‰) | Uncertainty | $\Delta^{14}C$ adjusted to 2017 | $CO_{2ff}$ (ppm) |
|---|---|---|---|---|---|---|---|---|---|
| 15 | IUACD#20C3032 | I3 | IUAC, New Delhi (2017) | 28°31′39″N, 77°10′7″E | Campus site | –29.90 | 1.95 | | 16.38 |
| 16 | IUACD#20C3007 | GGM | Huda City Centre, Gurugram (2018) | 28°27′37.38″N, 77°04′23.26″E | Children's park | 6.64 | 2.42 | 9.14 | 0.22 |
| 17 | IUACD#20C3009 | ANV | Anand Vihar Railway Station (2018) | 28°38′46.32″N, 77°18′57.82″E | Site near a railway station | 3.11 | 2.22 | 5.61 | 1.63 |
| 18 | IUACD#20C3019 | DU1 | Near Back Gate of Arts Faculty, Delhi University (2018) | 28°41′22.704″N, 77°12′26.064″E | Campus site | –15.62 | 1.83 | –13.12 | 9.28 |
| 19 | IUACD#20C3028 | NCC | Noida City Centre (2018) | 28°34′23.06″N, 77°21′21.14″E | School campus site | –23.14 | 1.78 | –20.64 | 12.43 |
| 20 | IUACD#20C3030 | FDB | Old Faridabad Metro Station (2018) | 28°24′34.27″N, 77°18′42.27″E | Site near a busy road | –51.84 | 1.63 | –49.34 | 24.91 |
| 21 | IUACD#20C3031 | NAR | Ghogha Village, Narela (2018) | 28°49′41.02″N, 77°03′11.68″E | Suburban site | –36.64 | 1.73 | –34.14 | 18.21 |
| 22 | IUACD#20C3035 | SNM | Sarojani Nagar Market (2018) | 28°34′36.68″N, 77°11′47.85″E | Crowded market site | –29.51 | 1.94 | –27.01 | 15.13 |
| 23 | IUACD#20C3038 | GZB | Khajuri Park, Ghaziabad (2018) | 28°40′50.59″N, 77°20′37.41″E | Park site | –74.62 | 1.64 | –72.12 | 35.37 |
| 24 | IUACD#20C3039 | BAW | Puth Khurd, Bawana, North West Delhi (2018) | 28°46′15.46″N, 77°02′13.47″E | Suburban site | –24.92 | 1.66 | –22.42 | 13.18 |
| 25 | IUACD#20C3041 | DTU | Delhi Technological University (2018) | 28°45′04.41″N, 77°07′02.87″E | Campus site | –14.97 | 1.83 | –12.47 | 9.01 |
| 26 | IUACD#20C3034 | SADB | Tis Hazari Metro Station (2020) | 28°40′02.76″N, 77°12′59.28″E | Parking area of a metro station | –61.2 | 2.15 | –51.93 | 26.08 |
| 27 | IUACD#20C3037 | CP | Connaught Place (2020) | 28°37′54.15″N, 77°13′03.20″E | Park site near a busy road | –44.26 | 1.63 | –34.96 | 18.56 |

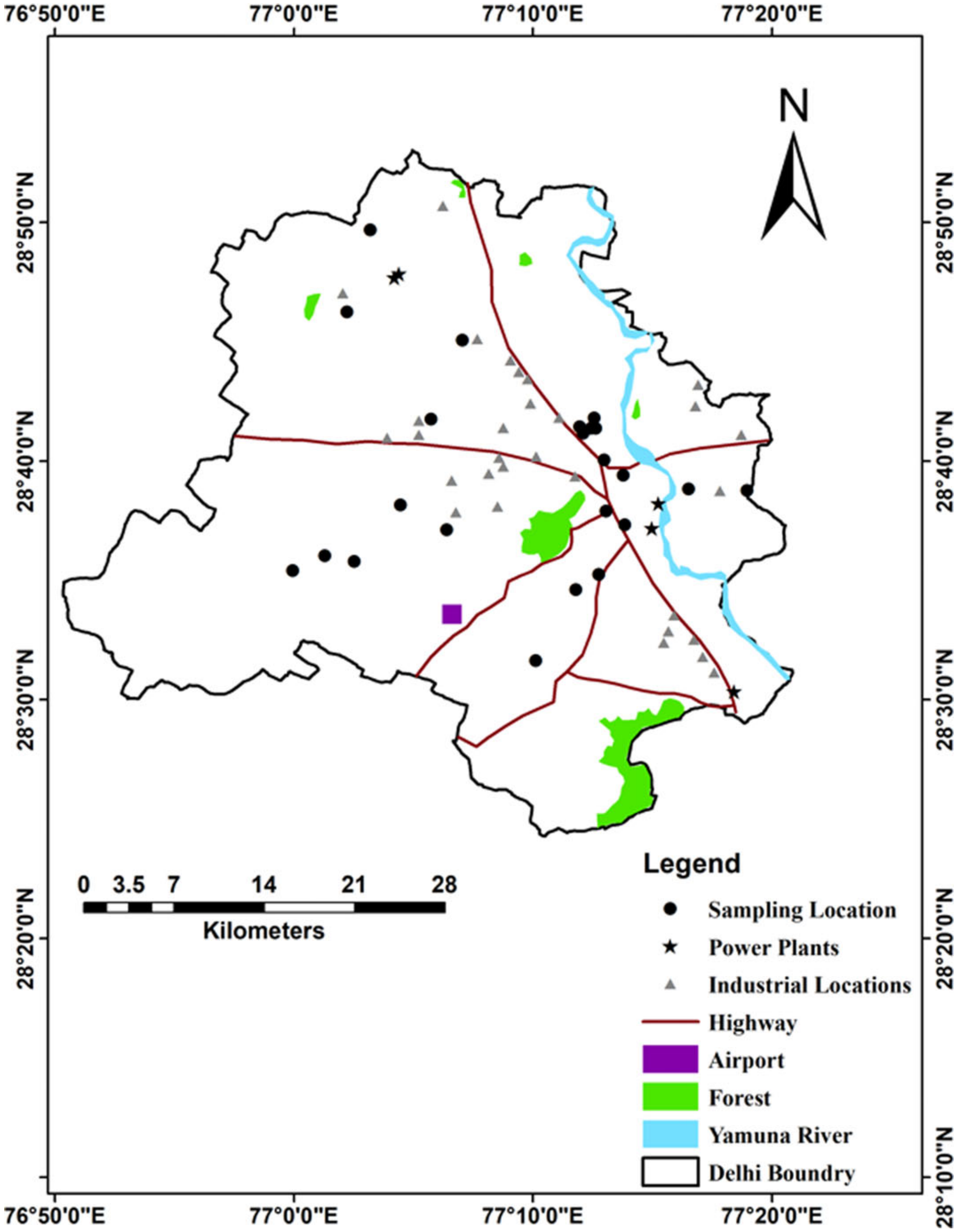


Figure 1 Study area and sampling locations.

### Sampling Sites and Sample Collection

For the present study, we collected and analyzed a total of 27 Peepal tree (*Ficus religiosa*) leave samples from 23 locations across megacity Delhi and four locations from adjacent cities i.e., Ghaziabad, Noida, Faridabad, and Gurugram (one sample from each city). Fifteen samples

https://doi.org/10.1017/RDC.2023.66 Published online by Cambridge University Press

were collected in the year 2017, 10 samples were collected in 2018, and 2 samples were collected in 2020. The Peepal tree was chosen for this study because it is the fourth most abundant tree species in Delhi's National Capital Territory (isfr vol. 2, 2019) and is found in the majority of the megacity and surrounding cities. It is a deciduous tree that sheds its leaves only once a year in March and April and new leaves start growing after 1–2 weeks and fully grown within a ~10-day period. Newly grown leaves are pink in color when they first emerge and convert into a dark green color after maturity. We collected mature leaves in the month of March. They represent the $CO_{2ff}$ signal for their growing period from April to March. The height of a Peepal tree can reach up to 30 m. We sampled leaves from 2 m above the ground. At this sampling height, leaves will be less influenced by soil respiration. From one sampling location, two–three leaves per tree were collected. Six of the 27 sampling sites are educational/research institute campuses, and 10 are parks in various areas of Delhi. Markets, metro station parking areas, roadside, suburban, and residential areas are among the remaining sampling locations. All the details of sampling sites including the collection time periods are given in Table 1, and sampling sites are shown in Figure 1.

### Sample Pretreatment, Graphitization, and $^{14}C$ Measurements

Sample pretreatment, graphitization, and $^{14}C$ measurements were performed at the accelerator mass spectrometry (AMS) facility of Inter University Accelerator Centre (IUAC), New Delhi (Sharma et al. 2019). Peepal tree leaves from one sampling location were dried and ground together. The mixture of tree leaves was pretreated using an acid-base-acid (ABA) protocol. In the first step, samples were treated with 0.5M HCl and then treated with 0.1M NaOH. In the final step, samples were again pretreated with 0.5 M HCl. In all the steps, samples were kept at 60°C temperature for 1-hr duration and rinsed with deionized water after each step. The pretreated samples were dried in a freeze dryer for 8–10 hr. 2.5–3 mg of each dried sample was packed into tin boats and combusted in an elemental analyzer at 920°C. The carbon dioxide produced was graphitized using automated graphitization equipment (AGE) (Sharma et al. 2019). $^{14}C$ in the graphite produced after graphitization was measured using a 500 kV Pelletron based accelerator mass spectrometer XCAMS (the $^{14}C$ accelerator mass spectrometer eXtended for $^{10}Be$ and $^{26}Al$) with a precision around 2‰. The $^{14}C/^{12}C$ ratio measured by XCAMS was normalized to the Oxalic Acid II standard sample, and AMS online $\delta^{13}C$ values were used for the isotopic fractionation correction. An external uncertainty of 2.51‰ was determined in radiocarbon measurements using 18 IAEA C3 secondary standard samples measured during the same period.

### Calculation of $\Delta^{14}C$ and $CO_{2ff}$

Radiocarbon content is expressed in terms of $\Delta^{14}C$ that is defined as follows:

$$\Delta^{14}C = \left[\frac{\left(\frac{^{14}C}{^{12}C}\right)_{SN}}{\left(\frac{^{14}C}{^{12}C}\right)_{abs}} - 1\right] \times 1000 \tag{1}$$

where $(^{14}C/^{12}C)_{SN}$ is the measured $^{14}C/^{12}C$ ratio in the samples normalized with $\delta^{13}C$ value of –25‰ and $(^{14}C/^{12}C)_{abs}$ is the absolute ratio of $^{14}C$ standard sample corrected for fractionation and $^{14}C$ decay (Stuiver and Polach 1977).

The AMS system provides the $^{14}C/^{12}C$ ratio of the sample, and this ratio is converted into $\Delta^{14}C$ as per Equation (1). Using $\Delta^{14}C$ values, $CO_{2ff}$ is calculated using following formulation described in Turnbull et al. (2009):

https://doi.org/10.1017/RDC.2023.66 Published online by Cambridge University Press

$$CO_{2ff} = \frac{CO_{2bg}\left(\Delta^{14}C_{mes} - \Delta^{14}C_{bg}\right)}{\Delta^{14}C_{ff} - \Delta^{14}C_{mes}} - \frac{CO_{2oth}\left(\Delta^{14}C_{oth} - \Delta^{14}C_{mes}\right)}{\Delta^{14}C_{ff} - \Delta^{14}C_{mes}} \quad (2)$$

where $\Delta^{14}C_{mes}$ = $\Delta^{14}C$ measured in the Peepal tree leaves in this study

$\Delta^{14}C_{bg}$ = $\Delta^{14}C$ measured at clean air background site

$\Delta^{14}C_{ff}$ = –1000‰ ($\Delta^{14}C$ value of fossil fuels. Since $^{14}C$ is absent in the fossil fuels, therefore, putting $^{14}C$ values as zero in Equation (1) will give $\Delta^{14}C_{ff}$ = –1000‰)

$CO_{2bg}$ = $CO_2$ from a clean air background site

$CO_{2oth}$ and $\Delta^{14}C_{oth}$ = $CO_2$ and $\Delta^{14}C$ from other sources such as heterotopic respiration, nuclear reactors, ocean exchange.

The second term in Equation (2) is considered as a correction or bias from other sources in $CO_{2ff}$ value. For continental sites, corrections for $CO_2$ from ocean can be ignored. There are two nuclear reactors at the distance of 150 km and 580 km from Delhi and both are pressurized heavy water reactors (PHWR). Pressurized water reactors emit $^{14}C$ dominantly in the form of $^{14}CH_4$ (Varga et al. 2020b, 2021). Both of these reactors are also not in the upwind direction of Delhi and this correction can also be ignored. Another source of $^{14}C$ is respiration, and it can be divided into autotrophic and heterotrophic respiration. $CO_2$ emitted during autotrophic respiration is generally absorbed from recent atmosphere (< 1 yr old; Wenger et al. 2019). However, $CO_2$ emitted by heterotopic respiration may have carbon from older materials such as decaying biomass from the bomb $^{14}C$ period. This $CO_2$ may have large amount of $^{14}C$ in comparison of current atmosphere and may produce a bias in the $CO_{2ff}$ values. However, as per previous studies, ignoring this correction will produce 0.2–0.5 ppm of bias in our $CO_{2ff}$ values as estimated for mid-latitude Northern Hemisphere (Turnbull et al. 2016).

## RESULTS AND DISCUSSION

### Spatial Distribution of $\Delta^{14}C$ across Megacity Delhi

We have presented the distribution of $\Delta^{14}C$ values for all the samples collected across Delhi in Figure 2(a) and values are given in Table 1. In order to prepare a spatial distribution map of $\Delta^{14}C$, we have scaled down all $\Delta^{14}C$ values to the year 2017 because most of the samples were collected in this year. For the scaling factor, we have used decreasing rate of background $\Delta^{14}C$ data for NH zone 3 as suggested in Hua et al. (2022). Background $\Delta^{14}C$ data for NH zone 3 is decreasing at the rate of 2.5‰ and 3.4‰ from April 2017 to March 2018 and from April 2018 to March 2019, respectively. We have assumed the same rate of decrease of 3.4‰ from April 2019 to March 2020, since this background data is available up to 2019 only (Hua et al. 2022). Samples collected in 2018 are scale down by 2.5‰ while two samples collected in the first week of March 2020 are scale down by 9.3‰ for the year 2017.

$\Delta^{14}C$ values are varying from –67.78‰ to 5.61‰ in the megacity Delhi where highest value belongs to a site from Anand Vihar while lowest value belongs to a site from a public park from Geeta colony in East Delhi district. East Delhi district is densely populated area having the third largest population density (22,639 persons/km$^2$) of eleven districts of Delhi city as per

https://doi.org/10.1017/RDC.2023.66 Published online by Cambridge University Press

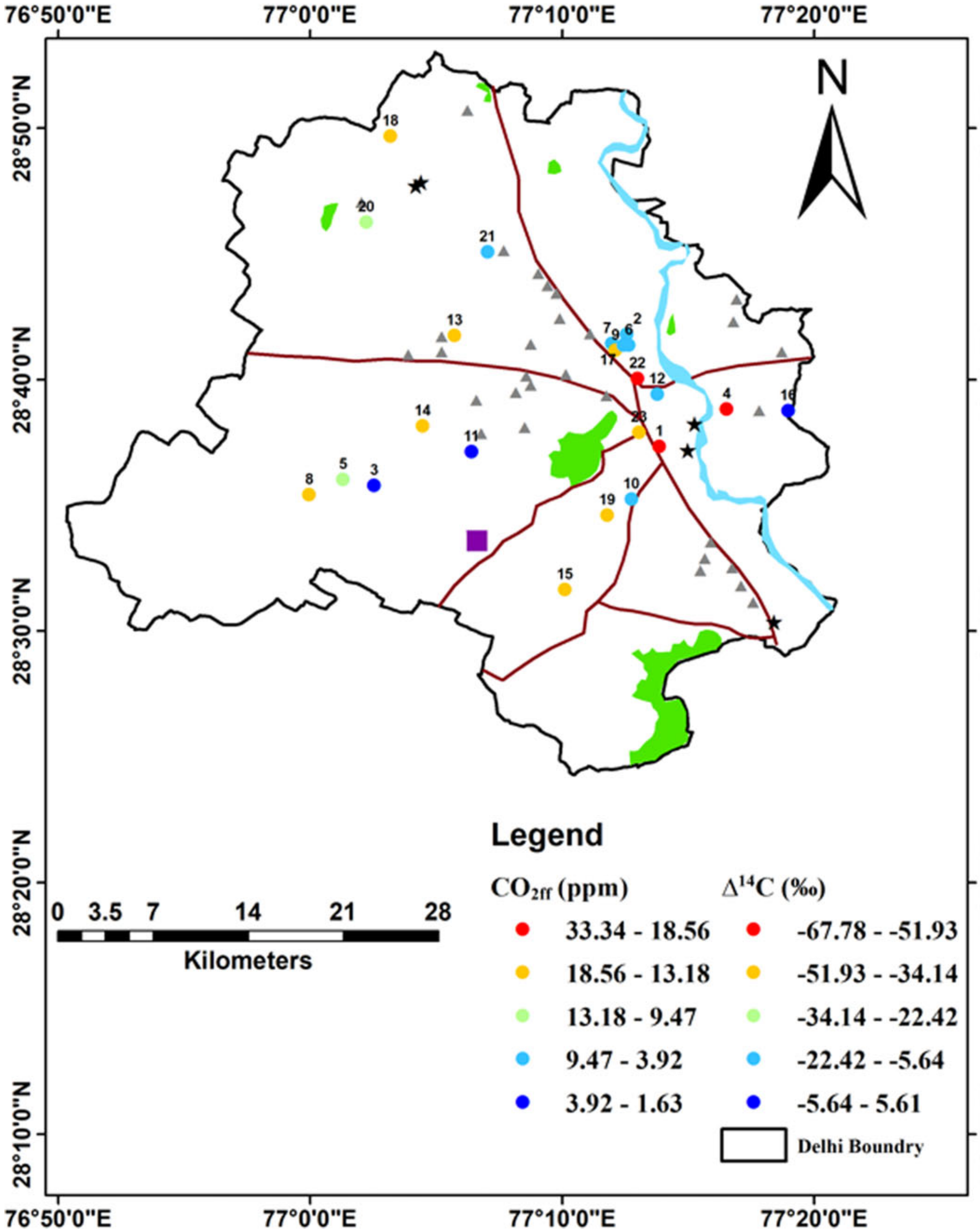


Figure 2 Spatial distribution of $\Delta^{14}C$ and $CO_{2ff}$ across megacity Delhi. Other legends of this figure are same as Figure 1.

2011 census. $\Delta^{14}C$ values for six campus sites are varying between –7.59‰ to 29.90‰. $\Delta^{14}C$ values are varying from 3.66‰ to –67.78‰ for the sampling sites located in the parks. As shown in Figure 2, we have observed depleted $\Delta^{14}C$ values from the sampling locations from Central Delhi (–47.17‰), the parking area of Tees Hazari Metro station (–51.93‰), Narela (34.14‰) and Sarojani nagar market (–27.01‰). Observed $\Delta^{14}C$ values in the four nearest

https://doi.org/10.1017/RDC.2023.66 Published online by Cambridge University Press

cities in the NCR region (Ghaziabad, Gurugram, Noida, and Faridabad) were found to be –69.62‰, 11.64‰, –18.14‰, and –46.84‰, and the $\Delta^{14}C$ values from nearest cities are not shown in Figure 2. They are given in Table 1.

### Selection of Background Site

We do not have $\Delta^{14}C$ values from a clean air background site in India. Therefore, we have utilized background values for Northern Hemisphere (NH) zone 3 reported in Hua et al. (2022). The present study region, Delhi, lies in the NH zone 3 as per the zones defined in Hua et al. (2022). We have taken average of $\Delta^{14}C$ values from April 2016 to March 2017 from this record for our study, and this average value is 9.7‰. For the $CO_{2bg}$ value, we used the average $CO_2$ value (401.12 ppm) from the observational station Nainital, India, from April 2016 to March 2017 (Nomura et al. 2021). Nainital (29.36ºN, 79.46ºE; 1940 m asl) is located at the bottom side of the Himalaya mountains and considered a background site for northern Indian air (Nomura et al. 2021).

### Spatial Distribution of $CO_{2ff}$ across Megacity Delhi

Using the Equation (2), the $CO_{2ff}$ values calculated for all collected samples across Delhi are given in Table 1, and spatial distribution map of $CO_{2ff}$ is presented in Figure 2. A maximum uncertainty of 1.18 ppm in $CO_{2ff}$ values of all samples can be derived from the corresponding external uncertainty of 2.51‰ in $^{14}C$ measurements.

The $CO_{2ff}$ values vary from 1.63 ppm to 33.34 ppm across megacity Delhi, and the highest value belongs to a site from a public park from Geeta colony in East Delhi district. $CO_{2ff}$ values for six campus sites vary between 6.99 ppm to 16.38 ppm with an average value of 10.22 ± 3.20 ppm (average value ± standard deviation). On the other hand, for the sampling sites located in the parks, the $CO_{2ff}$ values vary from 2.41 ppm to 33.34 ppm, with an average value of 13.32 ± 9.40 ppm. We have found campus sites to be more consistent than park sites, as seen from their standard deviation. This is because some parks sites are located in the densely populated areas (like Bhagat Singh park in East Delhi) and some parks are located with busy roads (e.g., sampling site in Connaught Place). $CO_{2ff}$ values for the four nearest cities in the NCR region (Ghaziabad, Gurugram, Noida, and Faridabad) are found to be 35.37 ppm, 0.22 ppm, 12.43 ppm, and 24.91 ppm, respectively. Figure 2 shows high $CO_{2ff}$ values in northwest Delhi, central Delhi, and parts of eastern Delhi and southwest Delhi. We also note that most of the industrial areas and four out of five thermal power plants are also situated in these parts of Delhi, as shown in Figures 1 and 2. Both thermal power plants and industrial areas are considered to be potential emission sources for fossil fuel $CO_2$.

The maximum value of $CO_{2ff}$ (33.34 ppm) observed in our study is higher than the maximum value observed in Rio de Janeiro state in Brazil (Santos et al. 2019) and Mexico City (Vay et al. 2009) but lower than the maximum value observed in Xi'an city (Zhou et al. 2014) as listed in Table 2. The $CO_{2ff}$ values in this study reflect the daytime fossil fuel $CO_2$ signal because photosynthesis occurs in the daytime only. $CO_{2ff}$ values may be higher during nighttime because of stable atmospheric conditions (Wang and Pataki 2010).

## SUMMARY AND CONCLUSIONS

Identifying the contribution of $CO_2$ emitted by fossil fuels would enable us to understand regional $CO_2$ budgets, particularly in urban areas, for any country. For the first time, we used

Table 2 Comparisons from similar studies.

| S. no. | Study area | Year of study | Maximum $CO_{2ff}$/range of $CO_{2ff}$ | Reference |
|---|---|---|---|---|
| 1 | Xi'an city, China | 2010 | 14.7 ± 1.7 to 52.6 ± 1.7 ppm | Zhou et al. 2014 |
| 2 | Rio de Janeiro state, Brazil | 2015–2016 | 27.6 ppm | Santos et al. 2019 |
| 3 | Mexico City, Mexico | 2006 | 4–15 ppm | Vay et al. 2009 |
| 4 | Delhi, India | 2016–2017 | 33.34 ppm | This study |

radiocarbon measurements at the city/urban scale to address the spatial distribution and quantify the contributions of $CO_{2ff}$ over different parts of the megacity Delhi region.

The main findings emerged from this study are as follows:

- We found that the spatial distribution of fossil fuel emissions is heterogeneous across megacity Delhi.
- $\Delta^{14}C$ values are varying between –67.78‰ to 5.61‰.
- $CO_{2ff}$ values are varying between 1.63 ppm to 33.34 ppm.
- Sampling sites located in the parks have larger $CO_{2ff}$ values (13.32 ± 9.40 ppm) than the sites located in the campuses (10.22 ± 3.20 ppm).

The present study emphasizes that Peepal tree leaves can be used to monitor fossil fuel $CO_2$ values in the absence of real-time monitoring of $CO_2$ values and can also aid in the establishment of future $CO_2$ monitoring stations in the Delhi region. Furthermore, this study provides the database for $CO_{2ff}$ in megacity Delhi that can be utilized for the mitigation policies.

## ACKNOWLEDGMENTS

Authors are thankful to IUAC for extending AMS facility for $^{14}C$ funded by Ministry of Earth Science (MoES), Govt. of India with reference numbers MoES/16/07/11(i)-RDEAS and MoES/P.O.(Seismic)8(09)-Geochron/2012. The authors would like to acknowledge the support of colleagues, collaborators, and friends for help with collection of samples.

## REFERENCES

Ahmad S, Baiocchi G, Creutzig F. 2015. $CO_2$ emissions from direct energy use of urban households in India. Environ. Sci. Technol. 49:11312–11320.

Andres RJ, Boden TA, Bréon FM, Ciais P, Davis S, Erickson D, Gregg JS, Jacobson A, Marland G, Miller J, Oda T, Olivier JGJ, Raupach MR, Rayner P, Treanton K. 2012. A synthesis of carbon dioxide emissions from fossil-fuel combustion, Biogeosciences 9:1845–1871.

Boden TA, Marland G, and Andres RJ. 2010. Global, regional, and national fossil-fuel CO2 emissions. Carbon Dioxide Information Analysis Center, Oak Ridge National Laboratory, U.S. Department of Energy, Oak Ridge, Tenn., U.S.A. doi: 10.3334/CDIAC/00001_V2010

Bozhinova D, Palstra S, Van der Molen M, Krol M, Meijer H, Peters W. 2016. Three years of $\Delta^{14}CO_2$ observations from maize leaves in the Netherlands and Western Europe. Radiocarbon 58(3): 459–478

Census. 2011. http://census2011.co.in [Indian census].

Chandra N, Lal S, Venkataramani S, Patra PK, Sheel V. 2016. Temporal variations of atmospheric $CO_2$ and CO at Ahmedabad in western India. Atmos. Chem. Phys. 16:6153–6173.

Ciais P, Sabine C, Bala G, Bopp L, Brovkin V, Canadell J, et al. 2013. Carbon and other biogeochem. In: Stocker TF, Qin D, Plattner G-K, et al., editors. Climate change 2013: the physical science basis. Contribution of Working Group I to the Fifth Assessment Report of the Intergovernmental Panel on Climate Change. Cambridge (UK) and New York: Cambridge University Press.

Delhi Economic Survey. 2021–2022. http://delhiplanning.nic.in/content/economic-survey-delhi-2021-22 [last accessed on 08/07/2022].

Duren RM, Miller CE. 2012. Measuring the carbon emissions of megacities. Nature Clim. Change 2:560–562.

Friedlingstein P, O'Sullivan M, Jones MW, Andrew RM, Hauck J, Olsen, et al. 2020. Global carbon budget 2020. Earth Syst. Sci. Data 12:3269–3340.

Hua Q, Turnbull JC, Santos GM, Rakowski AZ, Ancapichún S, De Pol-Holz R, Hammer S, Lehman SJ, Levin I, Miller JB, Palmer JG, Turney CSM. 2022. Atmospheric radiocarbon for the period 1950–2019. Radiocarbon 64(4):723–745.

Hsueh DY, Krakauer NY, Randerson JT, Xu XM, Trumbore SE, Southon JR. 2007. Regional patterns of radiocarbon and fossil fuel-derived $CO_2$ in surface air across North America, Geophys. Res. Lett. 34:L02816.

Indian State of Forest Report (ISFR). 2019. Volume 2. Published by Forest Survey of India (Ministry of Environment Forest and Climate Change). Dehradun, Uttarakhand, India https://fsi.nic.in/isfr19/vol2/isfr-2019-vol-ii-delhi.pdf [last accessed on 25/08/2021].

IPCC. 2014. Climate Change 2014: Synthesis Report. Contribution of Working Groups I, II and III to the Fifth Assessment Report of the Intergovernmental Panel on Climate Change [Core Writing Team, Pachauri RK, Meyer LA, editors]. Geneva, Switzerland: IPCC. 151 p.

Jain CD, Singh V, Akhil Raj ST, Madhavan BL, Ratnam MV. 2021. Local emission and long-range transport impacts on the CO, CO2, and $CH_4$ concentrations at a tropical rural site. Atm. Env. 254:11839

Kumar P, Gulia S, Harrison RM, Khare M. 2017. The influence of odd–even car trial on fine and coarse particles in Delhi. Environ. Pollut. 225: 20–30.

Lal S, Chandra N, Venkataramani S. 2015. A study of $CO_2$ and related trace gases using a laser-based technique at an urban site in western India. Current Science 109(11):2111–2116.

Levin I, Kromer B, Schmidt M, Sartorius H. 2003. A novel approach for independent budgeting of fossil fuel $CO_2$ over Europe by $^{14}CO_2$ observations. Geo-phys. Res. Lett. 30:2194.

Le Quéré C, Andrew RM, Friedlingstein P, Sitch S, Hauck J, Pongratz J, Pickers PA, et al. 2018. Global Carbon Budget 2018. Earth Syst. Sci. Data 10:2141–2194. doi: 10.5194/essd-10-2141-2018

Lichtfouse E, Lichtfouse M, Kashgarian M, Bol R. 2005. $^{14}C$ of grasses as an indicator of fossil fuel $CO_2$ pollution. Environ Chem Lett. 3:78–81.

Lin X, Indira NK, Ramonet M, Delmotte M, Ciais P, Bhatt BC, et al. 2015. Long-lived atmospheric trace gases measurements in flask samples from three stations in India, Atmos. Chem. Phys. 15:9819–9849.

Marland G, Boden TA, Andres RJ. 2003. Global, regional, and national $CO_2$ emissions. Trends: a compendium of data on global change. Oak Ridge (TN): Oak Ridge National Laboratory, U.S. Department of Energy. p. 34–43.

Mahato S, Pal S, Ghosh KG. 2020. Effect of lockdown amid COVID-19 pandemic on air quality of the megacity Delhi, India. Science of the Total Environment 730:139086.

Masood A, Ahmad K. 2023. Data-driven predictive modeling of $PM_{2.5}$ concentrations using machine learning and deep learning techniques: a case study of Delhi, India. Environ Monit Assess 195:60.

Metya A, Datye A, Chakraborty S, Tiwari YK, Sarma D, Bora A, Gogoi N. 2021. Diurnal and seasonal variability of $CO_2$ and $CH_4$ concentration in a semi-urban environment of western India. Sci Rep. 11:2931.

Niu Z, Zhou W, Wu S, Cheng P, Lu X, Xiong X, Du H, Fu Y, Wang G. 2016a. Atmospheric fossil fuel $CO_2$ traced by $\Delta^{14}C$ in Beijing and Xiamen, China: temporal variations, inland/coastal differences and influencing factors. Environ. Sci. Technol. 50:5474−5480

Niu Z, Zhou W, Zhang X, Wang S, Zhang D, Lu X, Cheng P, Wu S, Xiong X, Du H, Fu Y. 2016b. The spatial distribution of fossil fuel $CO_2$ traced by $\Delta^{14}C$ in the leaves of gingko (*Ginkgo biloba* L.) in Beijing City, China. Environ. Sci. Pollut. Res. 23(1):556–562.

Nomura S, Naja M, Ahmed MK, Mukai H, Terao Y, Machida T, Sasakawa M, Patra PK. 2021. Measurement report: Regional characteristics of seasonal and long-term variations in greenhouse gases at Nainital, India, and Comilla, Bangladesh, Atmos. Chem. Phys. 21:16427–16452.

Park JH, Hong W, Park G, Sung KS, Lee KH, Kim YE, Kim JK, Choi HW, Kim GD, Woo HJ. 2013. Distributions of fossil fuel originated $CO_2$ in five metropolitan areas of Korea (Seoul, Busan, Daegu, Daejeon, and Gwangju) according to the $\Delta^{14}C$ in ginkgo leaves. Nuclear Instruments and Methods in Physics ResearchB 294:508–514.

Riley WJ, Hsueh DY, Randerson JT, Fischer ML, Hatch JG, Pataki DE, Wang W, Goulden ML. 2008. Where do fossil fuel carbon dioxide emissions from California go? An analysis based on radiocarbon observations and an atmospheric transport model. J. Geophys. Res. 113:G04002.

Santos GM, Oliveira FM, Park J, Sena ACT, Chiquetto JB, Macario KD, Grainger CSG.

2019. Assessment of the regional fossil fuel $CO_2$ distribution through $\Delta^{14}C$ patterns in ipê leaves: the case of Rio de Janeiro state, Brazil. City and Environment Interactions 1:100001.

Seto KC, Dhakal S, Bigio A, Blanco H, Delgado GC, Dewar D, et al. 2014. Human settlements, infrastructure and spatial planning. Climate Change 2014: Mitigation of Climate Change. Contribution of Working Group III to the Fifth Assessment Report of the Intergovernmental Panel on Climate Change. Cambridge (UK) and New York: Cambridge University Press.

Sharma N, Dadhwal VK, Kant Y, Mahesh P, Mallikarjun K, Gadavi H, Sharma A, Ali MM. 2014. Atmospheric $CO_2$ variations in two contrasting environmental sites over India. Air, Soil and Water Research 7:61–68.

Sharma R, Kunchala R K, Ojha S, Kumar P, Gargari S, Chopra S. 2023. Spaial distribution of fossil fuel $CO_2$ across India using radiocarbon measurements in crop plants. Journal of Environmental Sciences 124:19–30.

Sharma R, Umapathy GR, Kumar P, Ojha S, Gargari S, Joshi R, Chopra S, Kanjilal D. 2019. AMS and upcoming geochronology facility at Inter University Accelerator Centre (IUAC), New Delhi, India. Nuclear Instruments and Methods in Physics Research B 438:124–130.

Sreenivas G, Mahesh P, Subin J, Kanchana AL, Rao PVN, Dadhwal VK. 2016. Influence of meteorology and interrelationship with greenhouse gases ($CO_2$ and $CH_4$) at a suburban site of India. Atmos. Chem. Phys. 16:3953–3967.

Stuiver M, Polach HA. 1977. Discussion: reporting of $^{14}C$ data. Radiocarbon 19:355–363.

Tiwari YK, Revadekar JV, Ravi KK. 2013. Variations in atmospheric carbon dioxide and its association with rainfall and vegetation over India. Atmospheric Environment 68:45–51.

Tiwari YK, Vellore RK, Ravi KK, van der Schoot M, Cho CH. 2014. Influence of monsoons on atmospheric $CO_2$ spatial variability and ground-based monitoring over India. Sci. Total Environ. 490:570–578.

Turnbull JC, Miller JB, Lehman SJ, Tans PP, Sparks RJ, Southon J. 2006. Comparison of $^{14}CO_2$, CO, and $SF_6$ as tracers for recently added fossil fuel $CO_2$ in the atmosphere and implications for biological $CO_2$ exchange. Geophys. Res. Lett. 33:L01817.

Turnbull J, Rayner P, Miller J, Naegler T, Ciais P, Cozic A. 2009. On the use of $^{14}CO_2$ as a tracer for fossil fuel $CO_2$: Quantifying uncertainties using an atmospheric transport model. J. Geophys. Res.-Atmos. 114:D22302.

Turnbull JC, Graven H, Krakauer NY. 2016. Radiocarbon in the atmosphere. In: Schuur E, Druffel E, Trumbore S, editors. Radiocarbon and climate change. Springer. p. 83–137.

Turnbull JC, Mikaloff Fletcher SE, Ansell I, Brailsford GW, Moss RC, Norris MW, Steinkamp K. 2017. Sixty years of radiocarbon dioxide measurements at Wellington, New Zealand: 1954–2014. Atmos. Chem. Phys. 17:14771–14784.

UN. 2014. United Nations Department of Economic and Social Affairs, Population Division. World Urbanization Prospects. The 2014 Revision, Highlights (ST/ESA/SER.A/352). New York: United Nations.

UN. 2018. United Nations Department of Economic Social Affairs, Population Division. World Urbanization Prospects. The 2018 Revision; online edition. New York: United Nations.

Varga T, Barnucz P, Major I, Lisztes-Szabó Z, Jull AJT, László E, Pénzes J, Molnár M. 2019. Fossil carbon load in urban vegetation for Debrecen, Hungary. Radiocarbon 61(5):1199–1210.

Varga T, Jull A, Lisztes-Szabó Z, Molnár M. 2020a. Spatial distribution of $^{14}C$ in tree leaves from Bali, Indonesia. Radiocarbon 62(1):235–242.

Varga T, Orsovszki G, Major I, Veres M, Bujtás T, Végh G, Manga L, Jull AJT, Palcsu L, Molnár M. 2020b. Advanced atmospheric $^{14}C$ monitoring around the Paks Nuclear Power Plant, Hungary. J. Environ. Radioact. 213:106138.

Varga T, Major I, Gergely V, Lencsés A, Bujtás T, Jull AJT, Veres M, Molnár M. 2021. Radiocarbon in the atmospheric gases and PM10 aerosol around the Paks Nuclear Power Plant, Hungary. J. Environ. Radioact. 237:106670.

Vay SA, Tyler SC, Choi Y, Blake DR, Blake NJ, Sachse GW, Diskin GS, Singh HB. 2009. Sources and transport of $\Delta^{14}C$ in $CO_2$ within the Mexico City Basin and vicinity. Atmos. Chem. Phys. 9:4973–4985.

Wenger A, Pugsley K, O'Doherty S, Rigby M, Manning AJ, Lunt MF, White ED. 2019. Atmospheric radiocarbon measurements to quantify $CO_2$ emissions in the UK from 2014 to 2015, Atmos. Chem. Phys. 19:14057–14070

Wang W, Pataki DE. 2010. Spatial patterns of plant isotope tracers in the Los Angeles urban region. Landscape Ecol 25: 35–52.

Wang P, Zhou W, Niu Z, Xiong X, Wu S, Cheng P, Hou Y, Lu X, Du H. 2021. Spatio-temporal variability of atmospheric $CO_2$ and its main causes: a case study in Xi'an city, China. Atmospheric Research 249:105346.

WHO. 2016. WHO Global Urban Ambient Air Pollution Database (Update 2016).

WMO. 2022: WMO Greenhouse Gas Bulletin. [Available online from https://library.wmo.int/doc_num.php?explnum_id=11352, last accessed on 21/03/2023].

Zhou W, Niu Z, Wu S, Xiong X, Hou Y, Wang P, Feng T, Cheng P, Du H, Lu X, An Z, Burr GS, Zhu Y. 2020. Fossil fuel $CO_2$ traced by radiocarbon in fifteen Chinese cities. Sci. Total Environ. 729:138639.

Zhou W, Wu S, Huo W, Xiong X, Cheng P, Lu X, Niu Z, 2014. Tracing fossil fuel $CO_2$ using $\Delta^{14}C$ inXi'an City, China. Atmos. Environ. 94: 538–545.